Macromolecular Research, Vol. 22, No. 6, pp 583-591 (2014)
DOI 10.1007/s13233-014-2085-y

www.springer.com/13233
pISSN 1598-5032 eISSN 2092-7673

Effects of Biodegradable Imidazolium-Based Ionic Liquid with Ester Group on the Structure and Properties of PLLA

Haoguan Gui[1], Yu Li[1], Shouyu Chen[1], Pei Xu[1], Bin Zheng[3], and Yunsheng Ding*[,1,2]

[1]*Institute of Polymer Materials & Chemical Engineering, School of Chemical Engineering, Hefei University of Technology, Hefei 230009, P. R. China*
[2]*Provincial Key Laboratory of Advanced Functional Materials and Devices, Hefei University of Technology, Hefei 230009, P. R. China*
[3]*Department of Chemistry and Chemical Engineering, Hefei Normal University, Hefei 230061, P. R. China*

Received July 3, 2013; Revised Februay 26, 2014; Accepted Februay 26, 2014

Abstract: Blends of poly(*L*-lactide) (PLLA) and a functional ionic liquid (IL), 3-methyl-1-(ethoxycarbonylethyl) imidazolium tetrafluoroborate ([AOEMIm][BF_4]) with various weight ratios were prepared by melt compounding and their interactions, compatibilities, processing characteristics, crystallization behaviors, mechanical properties and thermal degradation were investigated in this study. The interaction between PLLA and [AOEMIm][BF_4] was first studied by infrared spectroscopy (IR) investigation, and then the Flory-Huggins interaction parameter between PLLA and [AOEMIm][BF_4] was calculated. The compatibility was also supported by both sample appearance and scanning electron microscopy (SEM) results. Crystallization and melting conditions were obtained from differential scanning calorimetry (DSC), and the glass transition temperature (T_g) of PLLA showed a gradual decrease with the increasing addition of [AOEMIm][BF_4]. The balancing torque data were obtained by Haaker torque rheometry, and the molecular weight data of processed PLLA obtained by gel permeation chromatography (GPC) tests reflected a positive effect of [AOEMIm][BF_4] on the melt-processing of PLLA. A strong increase of the mechanical parameters of PLLA, such as the elongation at break and the impact strength, was observed with the incorporation of [AOEMIm][BF_4] up to the content of 7 phr (phr is the abbreviation for parts per hundreds of resin, n phr denoted n g IL/100 g PLLA), while the tensile strength decreased slightly. The thermal stability of PLLA took a sustained downward trend, with the increasing contents of [AOEMIm][BF_4] in its matrices, as presented from thermogravimetric analysis (TGA). PLLA blended with 5 phr [AOEMIm][BF_4] achieved excellent overall performance; as well, the mechanical properties improved considerably, and damage to the thermal stability was acceptable.

Keywords: poly(*L*-lactide), ionic liquid, plasticization effect, thermal degradation.

Introduction

Poly(*L*-lactide) (PLLA) as a biodegradable, bioabsorbable and renewably derived thermoplastic polymer has been extensively investigated during the last decade. Due to its excellent biocompatibility, processability and excellent mechanical properties, PLLA has been widely applied not only in the biomedical and pharmaceutical fields, but also in the commodities area. However, several drawbacks including brittleness, poor thermal resistant, low heat-distortion temperature and low crystallization rate have limited certain applications of PLLA.[1-3] Various methods have been adopted to modify PLLA, such as copolymerization,[4,5] surface modification[6] and blending with functional agents[7] or other polymers,[8,9] aiming to overcome the shortcomings. Among these strategies, blending with various types of additives, organic molecules,[10] inorganic fillers,[11,12] rubbery elastomers[13] *etc*., have proven to be effective to improve heat resistance, toughness and processability of PLLA. However, they all have different problems which precluded them from applications.

Ionic liquids (ILs) are salts generally composed of organic cation and inorganic anion which can exist as liquid at room temperature with extremely low volatility.[14] Recently, ILs have been shown to be a potential "green" media in many fields due to their low volatility, low melting points, high thermal stability, low flammability, and good compatibility with a variety of organic and inorganic materials.[15] Since more and more attention has been paid to environmental protection, ecotoxicity and biotoxicity of ILs especially biodegradable and biorenewable ILs should be taken into special consideration.[16] Several groups have attempted the usage of ILs as potential performance-enhanced additives for polymers as they showed

---

*Corresponding Author. E-mail: dingys@hfut.edu.cn

similar structures to traditional nucleating agents, plasticizers and antistatic agents. Research on ILs as polymer additives has so far focused on their potential as plasticizers and/or lubricants for poly(methyl methacrylate),[17,18] poly(vinyl chloride),[19] PLLA[20,21] and so on. However, as far as our best knowledge, the study on the effects of added ILs on PLLA, especially addition of biodegradable ILs, are not reported.

In this contribution, PLLA was melt-blended with one kind of biodegradable imidazolium-based IL, 3-methyl-1-(ethoxycarbonylethyl) imidazolium tetrafluoroborate, [AOEMIm][BF_4]. The effects of the added IL on the structure and properties of PLLA were studied using various characterization techniques. Although IL toxicity and biodegradability properties should be assessed on a case-by-case basis, the generalization has been made that more hydrophilic ILs (lipophilic ILs can disrupt cell membranes) tend to have a lower toxicity toward a range of diverse organisms.[22] This particular structure of IL was chosen on the basis that IL with ester group has low toxicity and is biodegradable. The effects of IL doped PLLA on the environmental toxicity will not be addressed here and will be presented elsewhere.

Experimental

Materials. Poly(*L*-lactide) (PLLA) used in this study was Natureworks product PLA2002D with density of 1.24 g/cm^3. The content of *L*-lactide was about 96 wt% and the residual monomer was less than 0.3 wt%. 3-methyl-1-(ethoxycarbonylethyl) imidazolium tetrafluoroborate [AOEMIm][BF_4] with molecular weight of 256 was supplied by Lanzhou Greenchem ILs company, China.

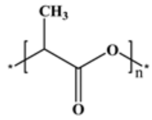

Poly(L-lactide)
PLLA

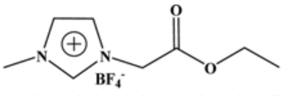

3-methyl-1-(ethoxycarbonylethyl)
imidazolium tetrafluoroborate
[AOEMIm][BF_4]

Preparation of Samples. Prior to melt-bending, PLLA pellets were dried in a desiccating dryer at 45 °C for 8 h, and ionic liquid was dried at 40 °C for 24 h in vacuum. The detailed description of the preparation of PLLA/ILs blends were presented as follows. First, PLLA was added in a Haake internal mixer at 170 °C till PLLA pellets fully melted, and then IL was added. These two components were continuously mixed for another 5 min. The mixing rollers were maintained at 30 rpm. The mass ratios of [AOEMIm][BF_4] in PLLA were 0, 1, 3, 5, 7, 9 phr, respectively, also note that "phr" is the abbreviation of "parts per hundreds of resins". Plate shape samples (1 mm thickness for tensile tests and 3 mm for Izod impact tests) were prepared by compression molding of PLLA samples in a plate vulcanizing machine. The nomenclature of PLLA materials in this study is presented in Table I.

Characterizations.

FTIR Spectroscopy: FTIR spectra of PLLA blends were collected on a Perkin-Elmer 100 IR spectrometer. Samples were pressed into transparent slices with a thickness of around 0.2 mm in a plate vulcanizing machine prior to the measurements.

Differential Scanning Calorimetry (DSC): DSC analysis was carried out by means of DSC, METTLER TOLEDO DSC821e, Switzerland, under nitrogen flow. (a) To study the effects of [AOEMIm][BF_4] on the thermal behaviors of PLLA, samples weighing 5-10 mg in the DSC apparatus were heated at 180 °C for 5 min, then quenched to 25 °C, and heated again to 180 °C at a rate of 10 °C/min. (b) To calculate the equilibrium melting point, samples were melted at 180 °C for 5 min, quickly cooled down to a given crystallization temperature and held for 90 min, then heated again to 200 °C at a rate of 10 °C/min to get the melting point.

Thermogravimetric Analysis (TGA): TGA curves of blends were recorded on Netzsch TG 209 F3 apparatus under nitrogen flow, linearly increased to 800 °C with a heating rate of 10 °C/min.

Table I. Sample Code of PLLA, PLLA/IL Samples, and Number Average Molecular Weight (M_n), Polydispersity (PDI), Balancing Torque and Appearance for Them

Sample Code	Proportions		M_n ($\times 10^4$)	PDI	Balancing Torque (N·m)	Appearance
	PLLA	IL				
PLLA	100	-	12.0±0.1	1.68±0.02	-	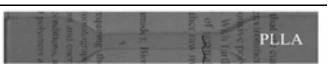
PLLA-0	100	-	9.8±0.3	1.84±0.04	11.6±0.1	
PLLA-1	100	1	9.7±0.3	1.88±0.07	10.5±0.3	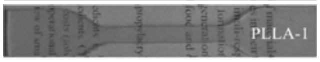
PLLA-3	100	3	9.7±0.4	1.78±0.06	9.5±0.2	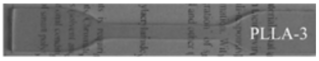
PLLA-5	100	5	11.1±0.2	1.76±0.02	6.1±0.4	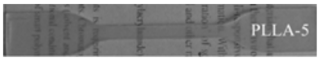
PLLA-7	100	7	11.6±0.2	1.82±0.04	4.7±0.3	
PLLA-9	100	9	11.7±0.1	1.77±0.03	3.7±0.1	

Gel Permeation Chromatography (GPC): GPC (Waters 1515 with Waters 2414 RI detector and isocratic HPLC pump, USA) was employed to examine molecular weight of PLLA before and after their processing by Haaker internal mixer. The samples for GPC measurements were obtained from tetrahydrofuran (THF) solutions of PLLA samples. THF was used as a fluent with a flow rate of 0.3 mL/min. The measuring temperature was set at 40 °C. Calibration of the measurements was based on polystyrene standards.

Scanning Electron Microscopy (SEM): The fractured surfaces of PLLA blends were coated with conductive gold layer and then observed by scanning electron microscope, JOEL JSM-6490LV.

Mechanical Property Measurements: Tensile properties of PLLA blends were measured by a universal tensile test machine at a tensile speed of 50 mm/min., in accordance to the standard ISO 527-1993. Izod impact measurements were conducted according to ISO 180-2000. Before tests, all blends were conditioned at 25 °C under a relative humidity of 50% for 3 days. The presented data were averaged over at least five measurements for each sample.

Results and Discussion

Interactions Between PLLA and IL. In order to investigate the interaction between PLLA and IL, FTIR spectra of PLLA, IL, PLLA-1, PLLA-5, PLLA-9, and PLLA-5 before and after extraction with ethanol for 24 h are depicted in Figure 1. There are remarkable differences between FTIR spectra of PLLA and PLLA/IL blends (shown in Figure 1(a)). The absorption bands at 1570 and 3160 cm^{-1} are attributed to the imidazole ring, which exists in IL and PLLA/IL blends. The areas of these bands increase with the IL content. However, it is found that the characteristic absorption bands at 1570 and 3160 cm^{-1} for the PLLA-5 disappeared after extraction with ethanol for 24 h (shown in Figure 1(b)). These results indicate the chemical-bond interaction between PLLA and IL is very limited.

To fully explain the interaction between PLLA and IL, the Flory-Huggins interaction parameter was calculated. Significant melting point depression was observed from the DSC data (discussed in 3.2). The measurements have been widely utilized to investigate polymer-polymer mixing thermodynamics.[23] The Flory-Huggins equation (eq. (1)) shows the relationship between the equilibrium melting point of pure polymer, $T^0_{m,pure}$, the depressed melting point, $T^0_{m,blend}$, and the Flory-Huggins interaction parameter, χ.[24] In this work, there were double endothermic peaks in the DSC curves of PLLA/IL blends (shown in Figure 4) due to melt-recrystallization-melt process, and the first endothermic peak (T_{m1}) was selected because it is directly related to the fusion of primary crystallites formed during the isothermal crystallization process. The equilibrium melting point of polymer can be calculated by Hoffman-Weeks equation (shown in Figure 2(a)) (eq. (2)).

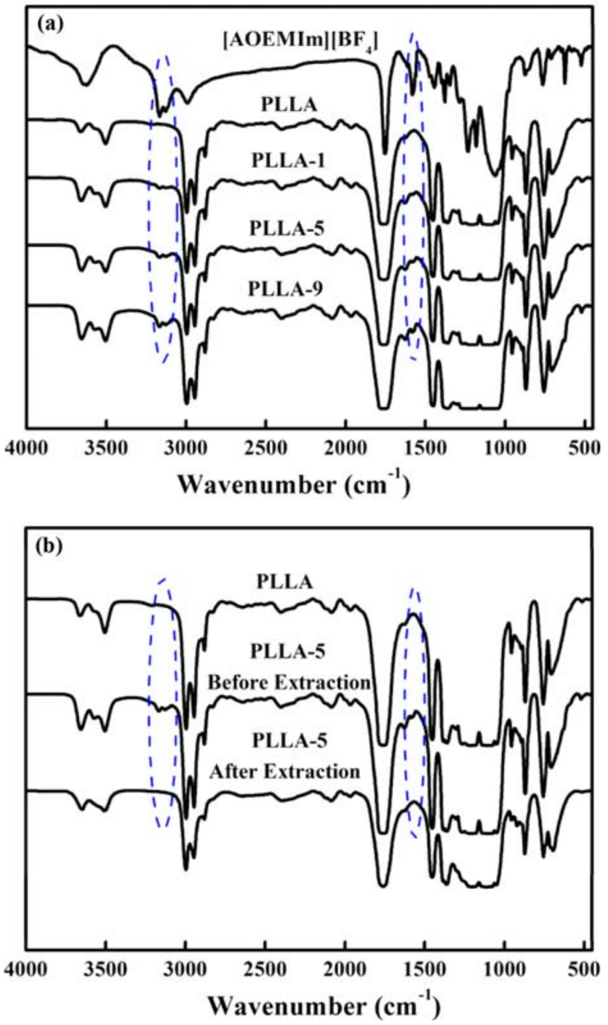

Figure 1. IR Spectra of PLLA, IL and PLLA/IL blends: (a) PLLA, IL and the PLLA blends by adding 1, 5, 9 phr IL; (b) PLLA , PLLA-5 before and after extraction with ethanol for 24 h.

$$\frac{1}{T^0_{m,blend}}-\frac{1}{T^0_{m,pure}}$$

$$=-\frac{R\cdot V_{2u}}{\Delta H_{2u}\cdot V_{1u}}\left[\frac{\ln\phi_2}{x_2}+\left(\frac{1}{x_2}-\frac{1}{x_1}\right)\cdot(1-\phi_2)+\chi_{12}\cdot(1-\phi_2)^2\right] \quad (1)$$

R -- Gas constant; V_u -- Molar volumes of polymer repeating unit; H_u -- Molar enthalpy of polymer repeating unit; -- Components volume fraction; x -- Degree of polymerization.

$$T^0_m - T_m = A(T^0_m - T_c) \quad (2)$$

T^0_m -- Equilibrium melting point; T_c -- A given crystallization temperature; T_m -- Melting point at T_c; A -- Crystal stability parameter.

When x_1=1, x_2=∞, the eq. (1) can be changed to eq. (3) which is suitable for PLLA/IL blends.

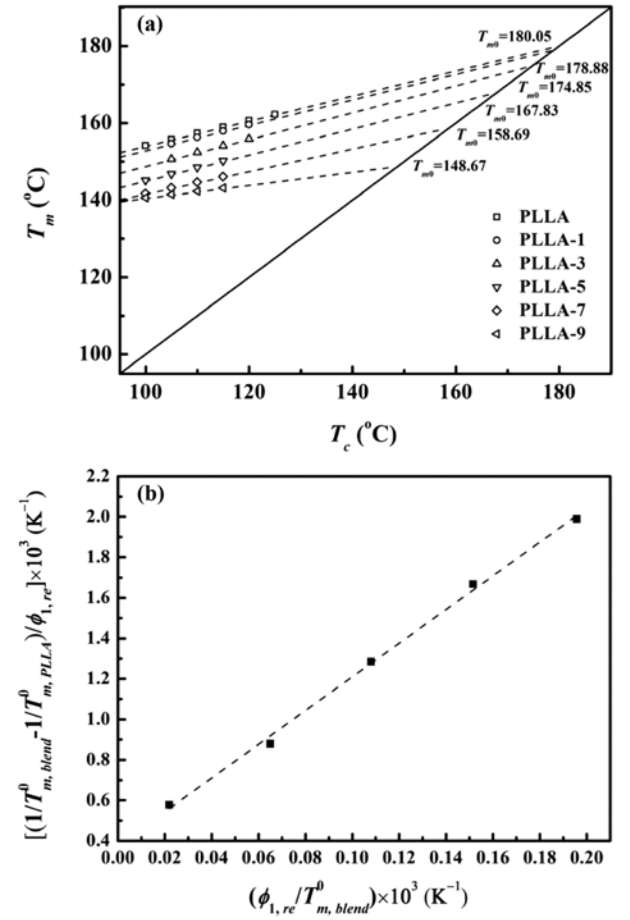

Figure 2. (a) The plot of Hoffman-Weeks; (b) a plot of quantity $(1/T^0_{m,blend}-1/T^0_{m,PLLA})/\phi_{1,re}$ against $\phi_{1,re}/T^0_{m,blend}$ for the PLLA/IL blends system, obtained according to eq. (5).

$$\frac{1}{T^0_{m,blend}}-\frac{1}{T^0_{m,pure}}=\frac{R\cdot V_{2u}}{\Delta H_{2u}\cdot V_{1u}}[(1-\phi_2)-\chi_{12}\cdot(1-\phi_2)^2] \qquad (3)$$

If ignoring the influence of volume and enthalpy, the Flory-Huggins interaction parameter can be indicated as eq. (4).

$$\chi_{12}=\frac{E\cdot V_{1u}}{RT} \qquad (4)$$

E -- Interaction energy of polymers.

Insertion of eq. (4) into eq. (3) gives

$$\frac{1}{\phi_1}\cdot\left(\frac{1}{T^0_{m,blend}}-\frac{1}{T^0_{m,pure}}\right)=-\frac{E\cdot V_{2u}}{\Delta H_{2u}}\cdot\frac{\phi_1}{T^0_{m,blend}}+\frac{R\cdot V_{2u}}{\Delta H_{2u}\cdot V_{1u}} \qquad (5)$$

With the eq. (5) the Flory-Huggins interaction parameter could be estimated as $\chi_{PLLA\text{-}IL}$= - 0.05 (170 °C) (shown in Figure 2(b)). It is apparent that the majority of the miscible systems have interactions parameters less than zero, indicating athermal or slightly exothermic mixing, which can prove the comparatively good compatibility between PLLA and [AOEMIm][BF$_4$] at the temperature 170 °C. The transparency of PLLA/IL blends prepared by melt processing remained unchanged, with only a slight yellowish tint versus the processed PLLA (shown in Table I). This can also suggest either thermodynamic miscibility of PLLA with the IL or an extremely fine dispersion at this particular IL concentration. Incompatibility of the IL with the amorphous transparent PLLA would be expected to result in opacity due to phase separation.

To further study the inherent interaction, the morphologies of PLLA and PLLA blends were also observed by SEM micrographs (shown in Figure 3). When the contents of IL in PLLA matrix are below 5 phr, small voids, corresponding to the etched IL components, can be found in micrographs, which are relatively homogeneously dispersed in the PLLA matrix.

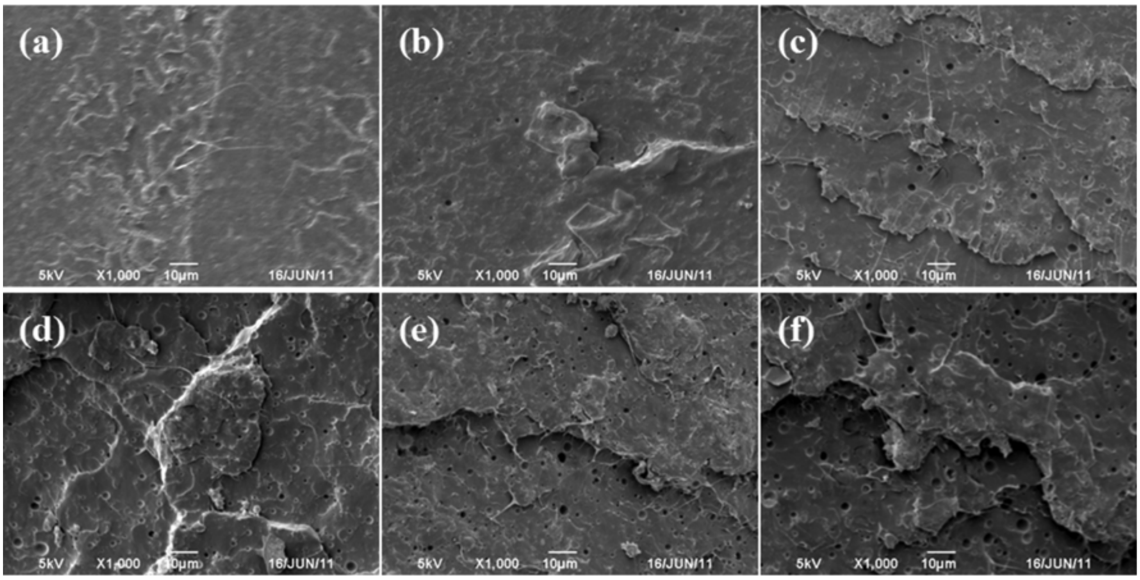

Figure 3. SEM micrographs of PLLA and PLLA/IL blends after etching with ethanol for 48 h: (a) PLLA; (b) PLLA-1; (c) PLLA-3; (d) PLLA-5; (e) PLLA-7; (f) PLLA-9.

As the contents of IL increase, average sizes of those voids increase apparently. Some large voids can be observed for blends with 7 and 9 phr IL due to the aggregation of IL. The reason is that IL is constituted of four fluoboric acid anion and one imidazolium-based cation, which has an ester group in its imidazole ring, and the polarity difference between PLLA and IL is very large. When the content of IL is relatively higher, IL will be aggregated resulting in phase separation.

Effects of IL on Thermal Behaviors of PLLA. Figure 4 presents the DSC heat flow curves during the second heating scan for PLLA and PLLA/IL blends. Only one single glass transition temperature (T_g) is observed for all PLLA/IL blends. As shown in Table II, PLLA/IL blends show a single T_g, lower than that of PLLA, which was found to decrease with increasing IL content. The amplitude of T_g depression lies between 56.1 °C (T_g of PLLA) and 50.1 °C (T_g of PLLA-9), showing an equally close performance to traditional plasticizers like glycerol and citrate ester.[25] The lowering of T_g suggests that IL have an effect on plasticizing. This plasticizing effect can be attributed to the following reasons. [AOEMIm][BF$_4$] is liquid and its polarity is relatively large even at room temperature (25 °C). When it is blended with PLLA and homogeneously dispersed in the PLLA matrix, it could weaken the interactions among PLLA chains leading to the decrease in PLLA chain cohesion acting as the diluents of PLLA chains, and eventually endow the higher mobility of PLLA chains.[18]

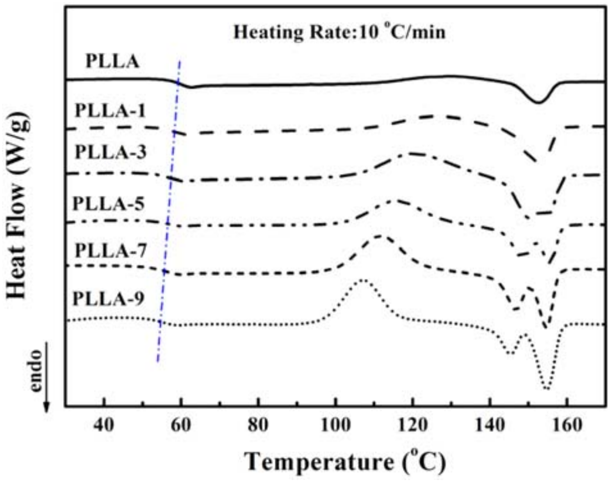

Figure 4. Second DSC heating flow curves for PLLA and PLLA/IL blends.

Table II. DSC Data of PLLA and PLLA/IL Blends[a] (Second Heating with a Heating Rate of 10 °C·min^{-1})

Sample Code	T_g (°C)	T_{cc} (°C)	ΔH_{cc} (J/g)	X_c (%)
PLLA	56.1	130.0	0.9	1.1
PLLA-1	54.5	129.0	8.7	10.7
PLLA-3	53.3	125.5	15.6	19.2
PLLA-5	52.9	120.5	27.6	33.9
PLLA-7	51.3	111.5	27.6	33.9
PLLA-9	50.1	107.0	30.0	36.9

[a] The reported enthalpy value for PLLA with 100% crystallinity is 93 J·g^{-1}.

From the DSC heating flow curve for PLLA during the second heating scan shown in Figure 4, a sick cold crystallization peak and weak melting peak can be observed which illuminate the poor crystallization ability of PLLA. On the contrast, different sizes of cold crystallization peaks and correspondingly intense melting peaks can be obtained from the DSC curves for PLLA/IL blends. This indicates that the existence of ILs can increase the crystallization rate of PLLA to a certain extent.

In addition, to observe the process of PLLA crystallization as well as to compare the influences of different samples on nucleation and crystallization, polarized optical microscope (POM) was adopted for the isothermal crystallization process of PLLA blends observation. Figure 4 presented the POM micrographs of PLLA and PLLA-3 during isothermal crystallization at 120 °C. As shown in Figure 5, the nucleation density of PLLA is very small while that of PLLA-3 enhances enormously. Because the PLLA/IL blends are not a fully compatible system, the existed interfaces will reduce the nucleation free energy of PLLA. That is, IL acts as the nucleating agent and changes the nucleation mode of PLLA. After nucleation, the embryos will slowly grow bigger to spherulites, but the radii of spherulites only get to approximately 50 μm for 60 min at 120 °C, which is close to the temperature of the fastest spherulitic growth rate, so it indicates the spherulitic growth rates of PLLA employed in this experiment are very slow. Furthermore, by comparing the spherulites radii of different samples after 60 min, it is found that the average spherulitic radius of pristine PLLA is slightly smaller than that of PLLA containing IL. On the other hand, the spherulitic growth rate is bound up with the ability of chain movement and arrangement, which is often characterized by value of the cooling crystallization temperature (T_{cc}).

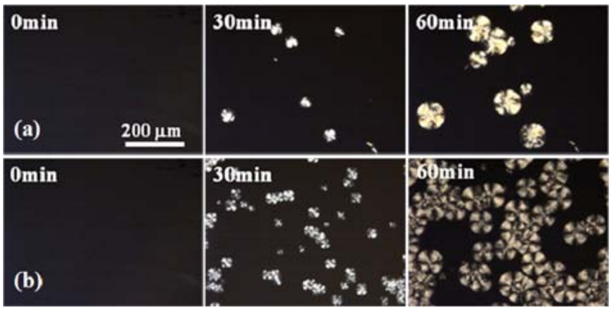

Figure 5. Selected POM micrographs for PLLA (a) and PLLA-3 (b) during isothermal crystallization at 120 °C. The labels refer to the time of isothermal crystallization. The scale bar represents 200 μm and is applied to all the micrographs.

Therefore, the above-mentioned result is in accordance with values of T_{cc} listed in Table II. The difference in the enthalpies of cold-crystallization (ΔH_{cc}) and crystallinity degree (X_c) for PLLA/IL blends from DSC analysis can be mainly attributed to the nucleation density and subordinately to spherulitic growth rate. Meanwhile the dispersing state of [AOEMIm][BF$_4$] in PLLA matrix on the cold-crystallizing process of PLLA cannot be ignored.

Effect of IL on the Processing of PLLA. The changes of balancing torque of PLLA/IL blends during melt blending are shown in Table I. The balancing torque of PLLA reaches the highest, while that of PLLA blends decreases gradually with the content of IL increasing. It suggests that IL can reduce the melt viscosity of PLLA during melt processing, which is related to the states of ILs during processing. When temperature is set at 170 ºC, IL is liquid and can act as lubricant and plasticizer, which is very helpful to improve the processing of PLLA.

The molecular weight of PLLA was also examined by GPC to evaluate the effect of IL on processing stability of PLLA. Table I lists the number average molecular weight (M_n) and polydispersity index (PDI) for unprocessed PLLA pellets, processed PLLA, and PLLA/IL blends. Compared with M_n of unprocessed PLLA, that of processed PLLA decreases enormously with about 16.7 percent loss. When the content of IL is low, M_n of the PLLA could be comparable to that of PLLA-0. The addition of 5 phr IL will slow down the decreasing rate of PLLA's M_n. Since the processing temperature of PLLA is 170 ºC which is only 20 ºC higher than the melting point and lower than 90 ºC (the onset decomposition temperature of PLLA at a heating rate of 30 ºC/min under nitrogen flow detected by TGA), the possibility of thermal degradation of PLLA during processing is very low. This suggests that PLLA experienced mechanical degradation mainly during the melt-mixing process due to shear, while PLLA blends added IL underwent relatively less mechanical degradation due to the lubricating and plasticizing effect of IL. The M_n of PLLA blends added with 1 and 3 phr IL are relatively lower, possibly due to the better compatibility between IL and PLLA, so IL could not play a significant lubricating role at its low contents. But with the increasing content of IL in PLLA, IL tends to aggregate, and the lubricating and plasticizing effects would be more obvious, corresponding to the less affection on the M_n for PLLA. In addition, the changes of PDI of PLLA have similar trends in this processing.

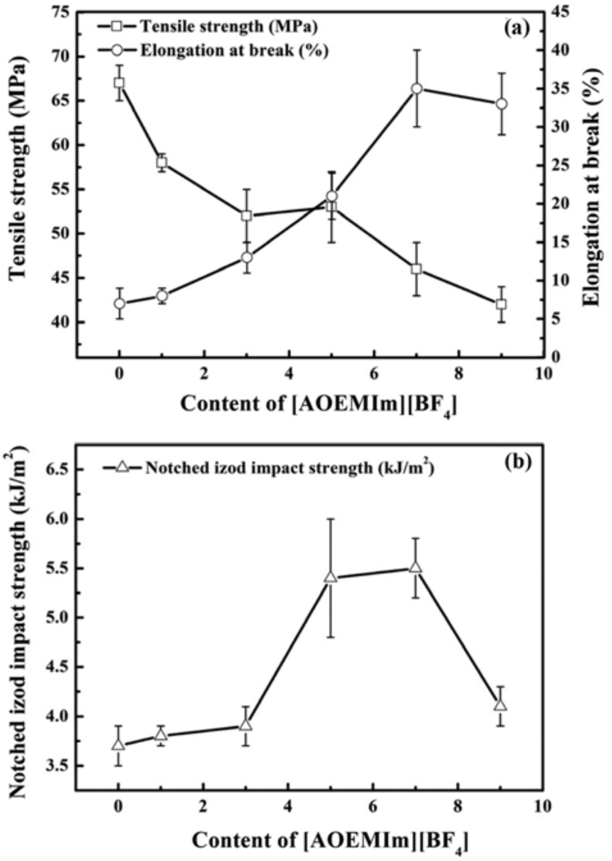

Figure 6. The mechanical properties of PLLA and PLLA/IL blends.

Effects of ILs on Mechanical Properties of PLLA. The mechanical properties of PLLA and PLL/IL blends are summarized in Figure 6. It can be found that the addition of IL leads to decrease of tensile strength of PLLA blends, while the elongation at break shows an obvious increase with respect to PLLA. The elongation at break for PLLA blends increases gradually when the content of IL in PLLA matrix increases up to 7 phr. This result is related to the dispersity of IL and crystallization of PLLA. On one hand, in low contents, IL not only could be dispersed in PLLA matrix with very small size (shown in Figure 1), but also acts as nucleating agent (shown in Figure 4) and could increase the degree of crystallization with large number of nuclei and small size of crystals. Therefore, these small sizes of IL and crystals could play an important role in absorption and transfer energy during tests, acting as stress buffer zones.[26] On the other hand, with the increase of crystallinity, the size of amorphous area will be smaller. Then the entanglement points in amorphous area will decrease, so the ability of chain motion would increase, causing elongation at break increasing.[27] However, the addition of 9 phr IL in the PLLA/IL blends will induce the aggregation of IL in PLLA forming defects and stress concentration points which will eventually cause the decrease of elongation at break, as well as the low crystallinity.

The PLLA blends with IL show relatively higher impact strengths than PLLA. The above discussions can be further confirmed by the following SEM micrographs of fractured surfaces after the izod impact tests.

The morphologies of fractured surfaces of PLLA blends by SEM are shown in Figure 7. PLLA sample exhibits smooth and continuous fracture surface corresponding to the absence of ductility, which indicates its fracture mode is predominantly brittle. A brittle-ductile transition at low IL contents

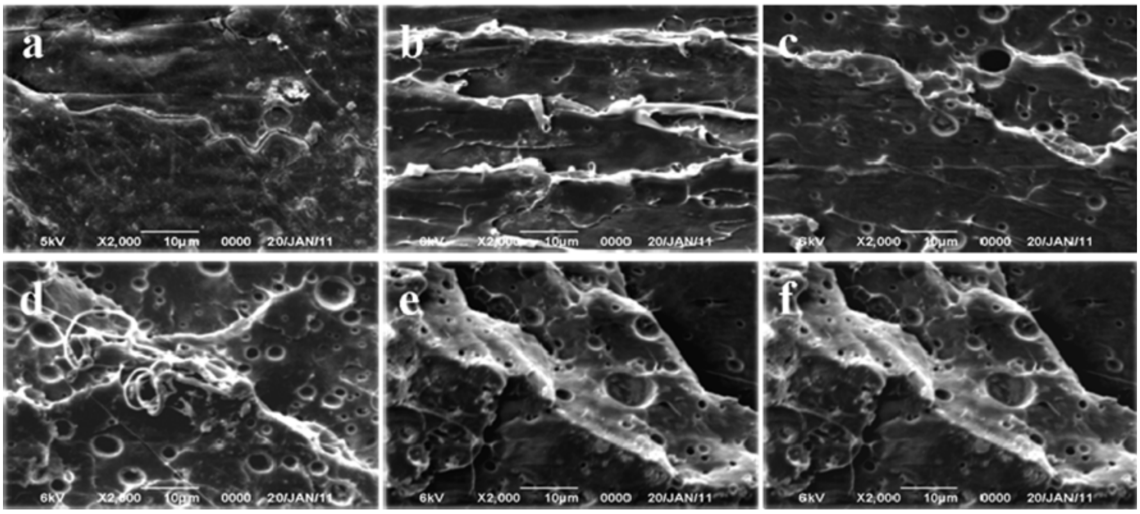

Figure 7. SEM micrographs of the fractured surfaces of PLLA and the PLLA/IL blends near the crack tip region after the izod impact tests. (a) PLLA; (b) PLLA-1; (c) PLLA-3; (d) PLLA-5; (e) PLLA-7; (f) PLLA-9.

can be deduced from the rougher fractured surfaces of the PLLA/IL blends with the increases of IL contents. Regarding the impact property, the inherent brittle deformation behavior of PLLA sample can be improved with the addition of IL, in which IL can be considered as toughening agents. Since the mechanical property of materials is closely related to the microscopic structures, other methods will be combined to further study.

Effects of IL on Thermal Degradation Behaviors of PLLA. TGA curves for PLLA and IL are shown in Figure 8. And, the onset decomposition temperatures (signified by 10% loss temperature, $T_{10\%}$), the corresponding temperatures of maximum decomposition rate (T_{max}) and the termination decomposition temperatures (signified by 90% loss temperature, $T_{90\%}$) of PLLA and blends with different contents of IL are summarized in Table III. It is observed that the thermal decomposition of IL undergoes two obvious processes due to the ester bond and imidazole ring in its structure.[28] The decomposition temperature of ester bond is lower than that of imidazole ring and the corresponding temperature of maximum decomposition rate (T_{max}) of ester bond of IL (334.6 °C) is lower than that of PLLA (356.5 °C).

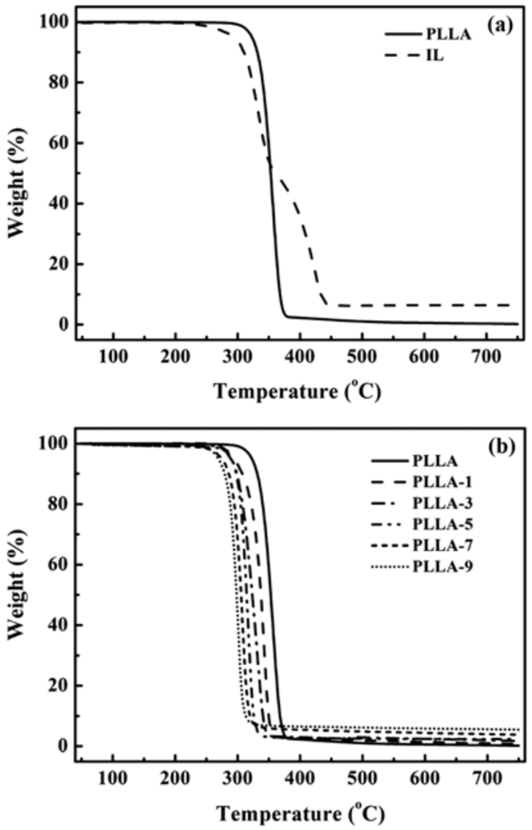

Figure 8. TGA curves for (a) PLLA and IL; (b) PLLA, PLLA-1, PLLA-3, PLLA-5, PLLA-7 and PLLA-9 at a heating rate of 10 °C·min^{-1}.

It is known that the average molecular weight and polydispersity have limited impacts on the thermal degradation of PLLA,[29,30] thus the effects of the molecular weight is ignored in this paper. The $T_{10\%}$, T_{max}, and $T_{90\%}$ of PLLA blends with IL are lower than PLLA (shown in Table III). This result suggests that IL cannot improve the thermal stability of PLLA at high temperatures. Xanthos and coworkers reported a similar phenomenon when using phosphonium-based ionic liquids to modify PLLA.[8,21] In order to study the influences of IL on PLLA thermal stability, the onset decomposition temperature ($T_{10\%}$) of every sample was analyzed and compared. It is interesting that $T_{10\%}$ of PLLA blends decreases with the increase of IL content, but the change becomes less notable and reaches stable values when the content of IL reached 5 phr. And the changes of T_{max} and $T_{90\%}$ have the similar trends. We had calculated the decreased values for these three char-

Table III. Decomposition Temperatures for PLLA and PLLA/IL Blends Determined from TGA at a Heating Rate of 10 °C·min^{-1}

Sample	$T_{10\%}$ (°C)	T_{max} (°C)	$T_{90\%}$ (°C)	Sample	$T_{10\%}$ (°C)	T_{max} (°C)	$T_{90\%}$ (°C)
PLLA	331.4	356.5	367.9	PLLA-3	298.8	332.4	340.5
[AOEMIm]BF$_4$	310.1	334.6 424.7	433.6	PLLA-5 PLLA-7	297.4 286.0	316.9 308.3	326.0 319.8
PLLA-1	307.5	343.1	349.7	PLLA-9	279.2	302.2	313.1

acteristic temperatures, and the largest is 50 °C for $T_{10\%}$, which is lower than the values reported by other researchers,[31] such as 70 °C or even much higher values. From the SEM micrographs in part 3.1, IL can be well mixed with PLLA when the content is 5 phr or lower, and IL will be oversaturated with the content increased to 7 phr or higher. The effect of IL on PLLA thermal decomposition may be in a surface reaction model. The catalytic efficiency is no longer significant advanced when the two-phase interface does not change.[32] In all, a new IL based additive has been doped into the PLLA system and the properties have been tested. With the addition of IL, the crystallization behavior, mechanical and processing properties have been improved. However, the drawback should never be neglected, such as the reduction of PLLA thermal stability. Therefore, in the future, the enhancement of properties with no loss of thermal stability should be further studied.

Conclusions

In this study, [AOEMIm][BF$_4$], one kind of IL with ester functional group was added in PLLA to evaluate its effects on the structure and properties of PLLA. [AOEMIm][BF$_4$] could be homogeneously dispersed in PLLA matrixes with the contents of 3 phr and 5 phr, and showed it partial miscibility with PLLA. The glass transition temperature (T_g) of PLLA lowered since the [AOEMIm][BF$_4$] incorporated into it indicating that it has effects of plasticizing to PLLA, while it could enhance the nucleating ability of PLLA. The [AOEMIm][BF$_4$] could hinder the degradation of PLLA which arisen by the mechanical scissor, and then the stability of PLLA increased effectively during its processing, but the thermal stability of PLLA decreased after [AOEMIm][BF$_4$] incorporating into it. The [AOEMIm][BF$_4$] could also lead to longer elongation at break as well as higher impact strength.

It is concluded that PLLA blends which consists of 5 phr [AOEMIm][BF$_4$] take a best overall performance. There is almost a balance between dispersion and agglomeration of 5 phr [AOEMIm][BF$_4$] in PLLA matrix, which result in more than 3 °C decreasing of T_g and less than 1×10^4 decreasing of M_n after the melt-blending process. And it exhibitd more than 200% increasing of elongation at break and 45% increasing of notched Izod impact strength, respectively. It cannot be ignored that the tensile strength and thermal stability of PLLA-5 are in a certain degree of expenditure. In summary, ionic liquids with tailorable structures should be potentially efficient and bio-degradable additives for PLLA.

Acknowledgment. This work is financially supported by Natural Science Foundation of China (50973025 and 51373045).

Supporting Information: Information is the differential scanning calorimetry (DSC) test to calculate the equilibrium melting point (T_m^0) for PLLA and PLLA/IL blends. The materials are available *via* the Internet at http://www.springer.com/13233.

References

(1) Y. Ikada and H. Tsuji, *Macromol. Rapid Commun.*, **21**, 117 (2000).
(2) R. A. Gross and B. Kalra, *Science*, **297**, 803 (2002).
(3) R. M. Rasal, A. V. Janorkar, and D. E. Hirt, *Prog. Polym. Sci.*, **35**, 338 (2010).
(4) H. Kim and S. Kim, *Macromol. Res.*, **19**, 448 (2011).
(5) T. Okuda, K. Ishimoto, H. Hitomi, and S. Shiro, *Macromolecules*, **45**, 4166 (2012).
(6) F. Poncin Epaillard, O. Shavdina, and D. Debarnot, *Mater. Sci. Eng., C*, **33**, 2526 (2013).
(7) M. Hakkarainen and A. F. Wistrand, *Update on Polylactide Based Materials*, iSmithers, Shawbury, Shrewsbury, GBR, 2011.
(8) M. Omura, T. Tsukegi, Y. Shirai, H. Nishida, and T. Endo, *Ind. Eng. Chem. Res.*, **45**, 2949 (2006).
(9) H. K. Jang and B. Kim, *Macromol. Res.*, **21**, 370 (2013).
(10) N. Burgos, V. P. Martino, and A. Jiménez, *Polym. Degrad. Stab.*, **98**, 651 (2013).
(11) J. W. Rhim, S. I. Hong, and C. S. Ha, *LWT - Food Sci. Technol.*, **42**, 612 (2009).
(12) Z. Antar, J. F. Feller, H. Noël, P. Glouannec, and K. Elleuch, *Mater. Lett.*, **67**, 210 (2012).
(13) D. Park, M. Kim, J. Yang, D. Lee, K. Kim, and B. Hong, W. Kim, *Macromol. Res.*, **19**, 105 (2011).
(14) R. D. Rogers and K. R. Seddon, *Science*, **302**, 792 (2003).
(15) S. Mallakpour and M. Dinari, in *Green Solvents II*, A. Mohammad and D. Inamuddin, Eds., Springer Netherlands 2012, pp 1-32.
(16) D. Zhao, Y. Liao, and Z. Zhang, *CLEAN - Soil, Air, Water*, **35**, 42 (2007).
(17) M. P. Scott, C. S. Brazel, M. G. Benton, J. W. Mays, J. D. Holbrey, and R. D. Rogers, *Chem. Commun.*, **13**, 1370 (2002).

(18) M. P. Scott, M. Rahman, and C.S. Brazel, *Eur. Polym. J.*, **39**, 1947 (2003).
(19) M. Rahman and C. S. Brazel, *Polym. Degrad. Stab.*, **91**, 3371 (2006).
(20) K. I. Park and M. Xanthos, *Polym. Degrad. Stab.*, **94**, 834 (2009).
(21) K. Park, J. U. Ha, and M. Xanthos, *Polym. Eng. Sci.*, **50**, 1105 (2010).
(22) S. P. M. Ventura, M. Gurbisz, M. Ghavre, F. M. M. Ferreira, F. Gonçalves, I. Beadham, B. Quilty, J. A. P. Coutinho, and N. Gathergood, *ACS Sustainable Chem. Eng.*, **1**, 393 (2013).
(23) E. Meaurio, E. Zuza, and J. R. Sarasua, *Macromolecules*, **38**, 1207 (2005).
(24) P. J. Flory, *Principles of Polymer Chemistry*, Cornell University Press, New York, 1953.
(25) O. Martin and L. Avérous, *Polymer*, **42**, 6209 (2001).
(26) H. Bai, H. Xiu, J. Gao, H. Deng, Q. Zhang, M. Yang, and Q. Fu, *ACS Appl. Mater. Interfaces*, **4**, 897 (2012).
(27) L. Corté and L. Leibler, *Macromolecules*, **40**, 5606 (2007).
(28) H. L. Ngo, K. LeCompte, L. Hargens, and A. B. McEwen, *Thermochim. Acta*, **357**, 97 (2000).
(29) P. Degée, P. Dubois, and R. Jérôme, *Macromol. Chem. Phys.*, **198**, 1985 (1997).
(30) F. Carrasco, P. Pagès, J. Gámez-Pérez, O. O. Santana, and M. L. Maspoch, *Polym. Degrad. Stab.*, **95**, 116 (2010).
(31) M.-F. Chiang, M.-Z. Chu, and T.-M. Wu, *Polym. Degrad. Stab.*, **96**, 60 (2011).
(32) T. Welton, *Coord. Chem. Rev.*, **248**, 2459 (2004).